PERGAMON

International Journal of Solids and Structures 38 (2001) 7885–7897

INTERNATIONAL JOURNAL OF SOLIDS and STRUCTURES

www.elsevier.com/locate/ijsolstr

Active damping of beams by piezoelectric system: effects of bonding layer properties

Marek Pietrzakowski *

Institute of Machine Design Fundamentals, Warsaw University of Technology, Narbutta 84, 02-524 Warszawa, Poland

Received 17 August 2000; in revised form 26 April 2001

Abstract

The paper is aimed at the active damping of structural vibration of a simply supported beam by using a piezoelectric, collocated sensor/actuator pair. The control concept is based on the velocity feedback. The bending-extensional dynamic model of the beam with glued piezoelements is proposed. The shear bonding layers both for the actuator and the sensor are assumed visco-elastic described by the Kelvin–Voigt material. The steady-state response of the beam loaded by a harmonic concentrated force is obtained from the solution of the boundary value problem. The boundary problem is formulated by the governing equations for the sections with and without piezoelectric patches, boundary conditions at the ends of the beam, continuity conditions between sections and the free stress conditions at the actuator and sensor edges. The influence of bonding layer parameters on the dynamic response of the controlled beam is analysed. The results in terms of frequency response of the beam transverse displacements show that the stiffness of bonding layers affects significantly the active damping efficiency. The beam vibrations can be reduced considerably for relatively stiff glue layers. The range of material damping parameter of the bonding layer, which causes an increase in the resonant amplitudes, is also indicated. A growth of stiffness as well as passive damping of the bonding layer results in a slight increase of resonance frequencies. The effect of variations in the bonding layer parameters on the shear stress distribution along the sensor and actuator is also presented and discussed.

Keywords: Active damping; Piezoelectric sensor/actuator; Bonding layer; Frequency response

1. Introduction

Piezoelectric materials have become popular in many engineering applications. Distributed sensors and actuators integrated with the flexible structure have been applied successfully in the closed-loop control (cf. Bailey and Hubbard, 1985; Alberts and Colvin, 1991; Newman, 1991; Dimitriadis et al., 1991; Lee et al., 1991). Dynamic analysis of the system is commonly based on the static relations describing an interaction between the perfectly bonded actuator and the substructure. A comprehensive static coupling model, which includes an elastic bonding layer, was analysed by Crawley and de Luis (1987). The dynamic approach for a simply supported beam with perfectly bonded actuators was presented by Pan et al. (1991). In their model

* Tel.: +48-22-660-86-23; fax: +48-22-660-86-22.
E-mail address: mpietrz@simr.pw.edu.pl (M. Pietrzakowski).

0020-7683/01/$ - see front matter
PII: S0020-7683(01)00105-6

the actuator extension with inertia forces was considered. Tylikowski (1993) formulated the dynamic bending-extensional model including the bonding layer with the finite shearing stiffness. This approach was applied to active damping of beams (Pietrzakowski, 1997) and stabilisation of beam parametric vibrations (Tylikowski, 1999). The comparison of the coupling models presented by Pietrzakowski (2000) shows that the static approximation is reasonable only for the sufficiently thin piezoelements and stiff glue layers when the dynamic interaction and shear effects can be neglected.

In the present study the developed bending-extensional model of a visco-elastic beam with a collocated sensor/actuator system is proposed. Taking into account a pure extension in piezoelements, the shear bonding layers both for the actuator and the sensor are assumed as visco-elastic and described by the Kelvin–Voigt material. The steady-state response of the beam excited by a harmonic concentrated force is obtained from the solution of the boundary value problem. The boundary problem is formulated by the dynamic equations for beam sections with and without piezoelectric patches, boundary conditions at the beam ends, continuity conditions between sections and the free stress conditions at the actuator and sensor edges. The purpose of the theoretical analysis is to show the influence of bonding layer parameters (elastic shear modulus and retardation time) on the dynamic response of the controlled beam.

2. Formulation of the problem and analysis

The considered system is a simply supported visco-elastic beam of the length l and width b loaded by the time-dependant force $F(t)$. Piezoelectric patches of the same width as the beam are mounted to both opposite sides of the beam, and form the collocated sensor/actuator pair. A voltage generated by the sensor and transformed according to the PD controller drives the actuator. For analysis the beam is divided into four parts due to the acting force cross-section and the location of piezoelectric device (Fig. 1). The dynamic behaviour of each part is governed by different equations. It is assumed that the massless bonding layers between the actuator as well as the sensor and the substructure are visco-elastic, described by the Kelvin–Voigt model.

2.1. Dynamic equations

The dynamic equations are formulated assuming bending of the beam agreeably to the Bernoulli–Euler theory, the longitudinal pure extension (compression) of piezoelements and pure one-dimensional shear in the bonding layers. The beam transverse displacement w and the longitudinal displacement u_a of the actuator and u_s of the sensor describe the motion of the system, respectively.

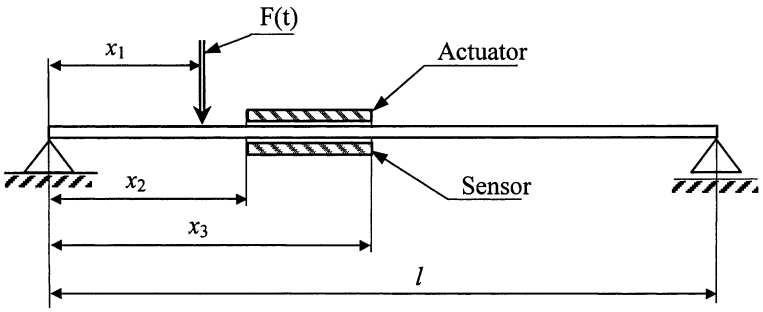

Fig. 1. Beam with a piezoelectric sensor/actuator pair.

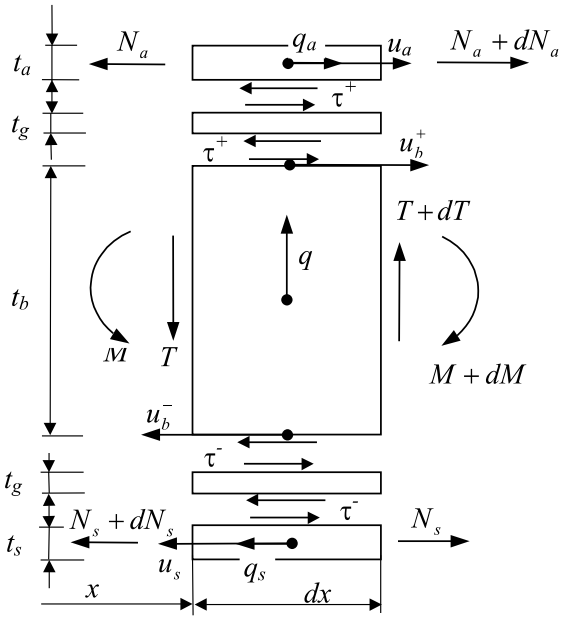

Fig. 2. Infinitesimal beam element with piezoelements and bonding layers.

The governing equations for the activated section of beam ($x_2 < x < x_3$) are derived considering an infinitesimal element shown in Fig. 2.

The longitudinal motion of the actuator and sensor is defined with inertial forces taking into account. Their intensities are $q_a = -\rho_a t_a b \frac{\partial^2 u_a}{\partial t^2}$ and $q_s = -\rho_s t_s b \frac{\partial^2 u_s}{\partial t^2}$, respectively. The governing equations can be expressed by strains $\varepsilon_a = \frac{\partial u_a}{\partial x}$ and $\varepsilon_s = \frac{\partial u_s}{\partial x}$ as follows:

$$E_a t_a \frac{\partial^2 \varepsilon_a}{\partial x^2} - \rho_a t_a \frac{\partial^2 \varepsilon_a}{\partial t^2} - \frac{\partial \tau^+}{\partial x} = 0 \tag{1}$$

$$E_s t_s \frac{\partial^2 \varepsilon_s}{\partial x^2} - \rho_s t_s \frac{\partial^2 \varepsilon_s}{\partial t^2} - \frac{\partial \tau^-}{\partial x} = 0 \tag{2}$$

where E_a, E_s, ρ_a, ρ_s, t_a, t_s denote Young's modulus, the mass density and thickness of the actuator and sensor, respectively. The shear stresses τ^+ and τ^- transmitted by the piezoelements are determined by stress–strain relations

$$\tau^+ = \frac{G_a^*}{t_g}\left(u_a - u_b^+\right) \tag{3}$$

$$\tau^- = \frac{G_s^*}{t_g}\left(u_s - u_b^-\right) \tag{4}$$

where u_b^+, u_b^- are the upper and lower beam surface longitudinal displacements, respectively; t_g is the bonding layer thickness; G_a^*, G_s^* are the linear functions of differential operator which for the Kelvin–Voigt model of bonding layer material can be written in the form

$$G_j^* = G_j\left(1 + \mu \frac{\partial}{\partial t}\right) \quad j = a, s \tag{5}$$

where G_j is Kirchhoff's modulus; μ is the retardation time (of the same value for each layer); the subscript $j = \mathrm{a}, \mathrm{s}$ refers to the actuator or sensor bonding layer, respectively.

The beam transverse motion is described by considering the dynamic coupling between the piezoelements and the beam, and also by including mass of piezoelements in the equivalent inertial force of intensity q (see Fig. 2). The beam governing equations are as follows:

$$\frac{\partial T}{\partial x} - \rho t_\mathrm{b} b \frac{\partial^2 w}{\partial t^2} = 0 \tag{6}$$

$$\frac{\partial M}{\partial x} - T + \frac{t_\mathrm{b} b}{2}(\tau^+ + \tau^-) = 0 \tag{7}$$

where T, M are the transverse force and bending moment, respectively; $\rho = (\rho_\mathrm{b} t_\mathrm{b} + \rho_\mathrm{a} t_\mathrm{a} + \rho_\mathrm{s} t_\mathrm{s})/t_\mathrm{b}$ is the equivalent mass density of activated section; t_b and ρ_b denote the thickness and mass density of beam, respectively.

Under the assumption of equal values of the upper and lower beam surface displacements, $u_\mathrm{b}^+ = u_\mathrm{b}^- = u_\mathrm{b}$, the following geometrical relations can be accepted

$$\frac{\partial^2 w}{\partial x^2} = -\frac{2}{t_\mathrm{b}} \frac{\partial u_\mathrm{b}}{\partial x} = -\frac{2}{t_\mathrm{b}} \varepsilon_\mathrm{b} \tag{8}$$

where ε_b is the beam surface extensional strain.

The bending moment in the beam cross-section described as a relation of the beam surface strain has the form

$$M = \frac{E_\mathrm{b}^* t_\mathrm{b}^2 b}{6} \varepsilon_\mathrm{b} \tag{9}$$

where $E_\mathrm{b}^* = E_\mathrm{b}\left(1 + \mu_\mathrm{b} \frac{\partial}{\partial t}\right)$ refers to the Kelvin–Voigt model of beam material with the following parameters: E_b – Young's modulus, μ_b – retardation time.

After eliminating shear stresses τ^+, τ^-, inner forces T, M, displacements u_b^+, u_b^- and w from the governing equations (1), (2) and (7), the motion of the actuator, sensor and beam can be expressed by strains ε_a, ε_s, ε_b in the system of coupled equations

$$E_\mathrm{a} t_\mathrm{a} \frac{\partial^2 \varepsilon_\mathrm{a}}{\partial x^2} - \frac{G_\mathrm{a}^*}{t_\mathrm{g}}(\varepsilon_\mathrm{a} - \varepsilon_\mathrm{b}) - \rho_\mathrm{a} t_\mathrm{a} \frac{\partial^2 \varepsilon_\mathrm{a}}{\partial t^2} = 0 \quad x \in (x_2, x_3) \tag{10}$$

$$E_\mathrm{s} t_\mathrm{s} \frac{\partial^2 \varepsilon_\mathrm{s}}{\partial x^2} - \frac{G_\mathrm{s}^*}{t_\mathrm{g}}(\varepsilon_\mathrm{s} - \varepsilon_\mathrm{b}) - \rho_\mathrm{s} t_\mathrm{s} \frac{\partial^2 \varepsilon_\mathrm{s}}{\partial t^2} = 0 \quad x \in (x_2, x_3) \tag{11}$$

$$\frac{E_\mathrm{b}^* t_\mathrm{b}^2}{12} \frac{\partial^4 \varepsilon_\mathrm{b}}{\partial x^4} + \frac{t_\mathrm{b}}{4}\left[\frac{G_\mathrm{a}^*}{t_\mathrm{g}}\left(\frac{\partial^2 \varepsilon_\mathrm{a}}{\partial x^2} - \frac{\partial^2 \varepsilon_\mathrm{b}}{\partial x^2}\right) + \frac{G_\mathrm{s}^*}{t_\mathrm{g}}\left(\frac{\partial^2 \varepsilon_\mathrm{s}}{\partial x^2} - \frac{\partial^2 \varepsilon_\mathrm{b}}{\partial x^2}\right)\right] + \rho \frac{\partial^2 \varepsilon_\mathrm{b}}{\partial t^2} = 0 \quad x \in (x_2, x_3) \tag{12}$$

The motion of other beam sections is described by the classical Bernoulli–Euler equation

$$\frac{E_\mathrm{b}^* t_\mathrm{b}^2}{12} \frac{\partial^4 \varepsilon_\mathrm{b}}{\partial x^4} + \rho_\mathrm{b} \frac{\partial^2 \varepsilon_\mathrm{b}}{\partial t^2} = 0 \quad x \in (0, x_1) \cup x \in (x_1, x_2) \cup x \in (x_3, l) \tag{13}$$

2.2. Piezoelectric sensor and actuator relations

The beam deflection develops the strain in the sensor. Due to the constitutive equation of piezoelectric material the electric displacement is as follows:

$$D_3 = -d_{31}^{s}\sigma_s \tag{14}$$

where d_{31}^{s} is the piezoelectric constant of sensor material; $\sigma_s = E_s\varepsilon_s$ is the sensor stress.

After integrating the charge over the sensor electrode area and applying the charge/voltage relation, the voltage produced by the sensor is equal to

$$V_s = C_s \int \varepsilon_s b_s(x)\,\mathrm{d}x \tag{15}$$

where $b_s(x) = b[H(x-x_2) - H(x-x_3)]$ denotes the sensor width distribution; $H(x)$ is the Heaviside function; C_s is the sensor constant of the form

$$C_s = d_{31}^{s} E_s \frac{t_s}{A_s e_{33}} \tag{16}$$

where $A_s = b(x_3 - x_2)$ is the sensor electrode area; e_{33} is the permittivity of sensor material.

Assuming that the sensor and actuator are electronically coupled with velocity feedback, the voltage applied to the actuator is given by

$$V_a = k_d \frac{\partial V_s}{\partial t} \tag{17}$$

where k_d is the gain factor of control loop.

The actuator constitutive strain–voltage relation has the form

$$\lambda = \frac{d_{31}^{a}}{t_a} V_a \tag{18}$$

where d_{31}^{a} is the piezoelectric constant of the actuator material.

The normal stresses σ_a, uniformly distributed in the actuator cross-section, are given by the following stress–strain relation

$$\sigma_a = E_a(\varepsilon_a - \lambda) \tag{19}$$

2.3. Boundary and continuity conditions

The equations of motion have to satisfy the simply supported boundary conditions at the beam ends at $x = 0$ and $x = l$, continuity of beam deflection, slope, curvature and transverse force at the borders of the sections at $x = x_1$, $x = x_2$, $x = x_3$ and free edge condition for the ends of both the actuator and the sensor.

The external force $F(t)$ acting at the cross-section $x = x_1$ imposes the following form of the continuity condition of transverse force:

$$\left.\frac{\partial \varepsilon_b}{\partial x}\right|_{x_1^-} = \left.\frac{\partial \varepsilon_b}{\partial x}\right|_{x_1^+} + \frac{6F}{E_b t_b^2 b} \tag{20}$$

The continuity of transverse force at the boundaries of activated part of the beam is found taking into account the shear stresses τ^+ and τ^- which are transmitted by the bonding layers. The following relations give the above condition in terms of strain:

for $x = x_2$

$$\frac{E_b^* t_b}{3}\left.\frac{\partial \varepsilon_b}{\partial x}\right|_{x_2^-} = \frac{E_b^* t_b}{3}\left.\frac{\partial \varepsilon_b}{\partial x}\right|_{x_2^+} + \frac{G_a^*}{t_g}\left(\int \varepsilon_a\,\mathrm{d}x - \int \varepsilon_b\,\mathrm{d}x\right)\Bigg|_{x_2^+} + \frac{G_s^*}{t_g}\left(\int \varepsilon_s\,\mathrm{d}x - \int \varepsilon_b\,\mathrm{d}x\right)\Bigg|_{x_2^+} \tag{21}$$

and for $x = x_3$

$$\frac{E_b^* t_b}{3}\frac{\partial \varepsilon_b}{\partial x}\bigg|_{x_3^-} + \frac{G_a^*}{t_g}\left(\int \varepsilon_a\,dx - \int \varepsilon_b\,dx\right)\bigg|_{x_3^-} + \frac{G_s^*}{t_g}\left(\int \varepsilon_s\,dx - \int \varepsilon_b\,dx\right)\bigg|_{x_3^-} = \frac{E_b^* t_b}{3}\frac{\partial \varepsilon_b}{\partial x}\bigg|_{x_3^+} \tag{22}$$

The free edge conditions at the actuator and sensor ends have to satisfy the zero normal stresses. Therefore, it requires according to the stress–strain relation (19) that for the actuator is

$$\varepsilon_a(x_2^+, t) = \varepsilon_a(x_3^-, t) = \lambda \tag{23}$$

where the piezoelectric strain λ is given by Eq. (18). The voltage supplying of the actuator is determined by Eq. (15) and the feedback rule, Eq. (17). The free ends conditions for the sensor yield

$$\varepsilon_s(x_2^+, t) = \varepsilon_s(x_3^-, t) = 0 \tag{24}$$

The boundary and continuity conditions can be written as the following system of equations:

$$w(0,t) = w(l,t) = 0 \tag{25}$$

$$\frac{\partial^2 w}{\partial x^2}\bigg|_{x=0} = \frac{\partial^2 w}{\partial x^2}\bigg|_{x=l} = 0 \tag{26}$$

$$w(x_1^-, t) = w(x_1^+, t) \quad w(x_2^-, t) = w(x_2^+, t) \quad w(x_3^-, t) = w(x_3^+, t) \tag{27}$$

$$\frac{\partial w}{\partial x}\bigg|_{x=x_1^-} = \frac{\partial w}{\partial x}\bigg|_{x=x_1^+} \quad \frac{\partial w}{\partial x}\bigg|_{x=x_2^-} = \frac{\partial w}{\partial x}\bigg|_{x=x_2^+} \quad \frac{\partial w}{\partial x}\bigg|_{x=x_3^-} = \frac{\partial w}{\partial x}\bigg|_{x=x_3^+} \tag{28}$$

$$\frac{\partial^2 w}{\partial x^2}\bigg|_{x=x_1^-} = \frac{\partial^2 w}{\partial x^2}\bigg|_{x=x_1^+} \quad \frac{\partial^2 w}{\partial x^2}\bigg|_{x=x_2^-} = \frac{\partial^2 w}{\partial x^2}\bigg|_{x=x_2^+} \quad \frac{\partial^2 w}{\partial x^2}\bigg|_{x=x_3^-} = \frac{\partial^2 w}{\partial x^2}\bigg|_{x=x_3^+} \tag{29}$$

$$T(x_1^-, t) = T(x_1^+, t) \quad T(x_2^-, t) = T(x_2^+, t) \quad T(x_3^-, t) = T(x_3^+, t) \tag{30}$$

$$\sigma_a(x_2^+, t) = \sigma_a(x_3^-, t) = 0 \quad \sigma_s(x_2^+, t) = \sigma_s(x_3^-, t) = 0 \tag{31}$$

The transverse displacement w one can eliminate from the above equations by applying the geometrical relation (8).

2.4. Steady-state solution

The equations of motion and the system of boundary conditions form the boundary value problem. The solution to it gives the dynamic strain response of the beam and piezoelements. The steady-state response is analysed. Therefore, it is assumed that the force acting on the beam is a harmonic single frequency function of amplitude F_0, $F(t) = F_0 \exp(i\omega t)$. The solutions of dynamic equations (Eqs. (10)–(13)) are harmonic with the same angular velocity as the excitation

$$\begin{bmatrix} \varepsilon_a(x,t) \\ \varepsilon_s(x,t) \\ \varepsilon_b(x,t) \end{bmatrix} = \begin{bmatrix} \varepsilon_a(x) \\ \varepsilon_s(x) \\ \varepsilon_b(x) \end{bmatrix} \exp(i\omega t) \tag{32}$$

Substituting the solutions Eq. (32) into the governing equations (Eqs. (10)–(13)), a system of ordinary differential equations is obtained. The solutions in the spatial domain have the form dependent on the section of the beam. The classical beam sections are described by

$$\varepsilon_b(x) = C_1 \exp(k_1 x) + C_2 \exp(-k_1 x) + C_3 \exp(ik_1 x) + C_4 \exp(-ik_1 x) \quad x \in (0, x_1) \tag{33}$$

$$\varepsilon_{\mathrm{b}}(x) = C_5 \exp(k_1 x) + C_6 \exp(-k_1 x) + C_7 \exp(\mathrm{i}k_1 x) + C_8 \exp(-\mathrm{i}k_1 x) \quad x \in (x_1, x_2) \tag{34}$$

$$\varepsilon_{\mathrm{b}}(x) = C_{17} \exp(k_1 x) + C_{18} \exp(-k_1 x) + C_{19} \exp(\mathrm{i}k_1 x) + C_{20} \exp(-\mathrm{i}k_1 x) \quad x \in (x_3, l) \tag{35}$$

where the wavenumber k_1 has the form

$$k_1 = \sqrt[4]{\frac{12\rho_{\mathrm{b}}\omega^2}{\hat{E}_{\mathrm{b}} t_{\mathrm{b}}^2}}$$

with $\hat{E}_k$ which indicates the complex Young modulus.

The activated beam section ($x_2 < x < x_3$) has the following solutions for the beam surface strain and actuator and sensor strains, respectively:

$$\varepsilon_{\mathrm{b}}(x) = \sum_{n=9}^{16} C_n \exp(k_n x) \tag{36}$$

$$\varepsilon_{\mathrm{a}}(x) = \sum_{n=9}^{16} \frac{C_n}{\alpha_{\mathrm{a}}(k_n, \omega)} \exp(k_n x) \tag{37}$$

$$\varepsilon_{\mathrm{s}}(x) = \sum_{n=9}^{16} \frac{C_n}{\alpha_{\mathrm{s}}(k_n, \omega)} \exp(k_n x) \tag{38}$$

where

$$\alpha_j(k_n, \omega) = 1 - \frac{E_j t_j t_{\mathrm{g}}}{\hat{G}_j} k_n^2 - \frac{\rho_j t_j t_{\mathrm{g}}}{\hat{G}_j} \omega^2 \quad j = \mathrm{a}, \mathrm{s}$$

with $\hat{G}_j$ ($j = a$, s) which is the Fourier transformation of the function, Eq. (5), describing adhesive material properties (complex shear modulus).

The wavenumbers $k_n = 9, \ldots, 16$ are calculated from the algebraic equation of the form

$$A_8 k_n^8 + A_6 k_n^6 + A_4 k_n^4 + A_2 k_n^2 + A_0 = 0 \tag{39}$$

where

$$A_8 = \frac{\hat{E}_{\mathrm{b}} t_{\mathrm{b}}^2}{12} E_{\mathrm{a}} t_{\mathrm{a}} E_{\mathrm{s}} t_{\mathrm{s}}$$

$$A_6 = \frac{\hat{E}_{\mathrm{b}} t_{\mathrm{b}}^2}{12} (\rho_{\mathrm{a}} t_{\mathrm{a}} E_{\mathrm{s}} t_{\mathrm{s}} + \rho_{\mathrm{s}} t_{\mathrm{s}} E_{\mathrm{a}} t_{\mathrm{a}}) \omega^2 - \frac{\hat{E}_{\mathrm{b}} t_{\mathrm{b}}^2}{12} \left(\frac{\hat{G}_{\mathrm{s}}}{t_{\mathrm{g}}} E_{\mathrm{a}} t_{\mathrm{a}} + \frac{\hat{G}_{\mathrm{a}}}{t_{\mathrm{g}}} E_{\mathrm{s}} t_{\mathrm{s}} \right) - \frac{t_{\mathrm{b}}}{4} \frac{\hat{G}_{\mathrm{a}} + \hat{G}_{\mathrm{s}}}{t_{\mathrm{g}}} E_{\mathrm{a}} t_{\mathrm{a}} E_{\mathrm{s}} t_{\mathrm{s}}$$

$$A_4 = \frac{\hat{E}_{\mathrm{b}} t_{\mathrm{b}}^2}{12} \rho_{\mathrm{a}} t_{\mathrm{a}} \rho_{\mathrm{s}} t_{\mathrm{s}} \omega^4 - \left[\frac{\hat{E}_{\mathrm{b}} t_{\mathrm{b}}^2}{12} \left(\frac{\hat{G}_{\mathrm{s}}}{t_{\mathrm{g}}} \rho_{\mathrm{a}} t_{\mathrm{a}} + \frac{\hat{G}_{\mathrm{a}}}{t_{\mathrm{g}}} \rho_{\mathrm{s}} t_{\mathrm{s}} \right) + \frac{t_{\mathrm{b}}}{4} \frac{\hat{G}_{\mathrm{a}} + \hat{G}_{\mathrm{s}}}{t_{\mathrm{g}}} (\rho_{\mathrm{a}} t_{\mathrm{a}} E_{\mathrm{s}} t_{\mathrm{s}} + \rho_{\mathrm{s}} t_{\mathrm{s}} E_{\mathrm{a}} t_{\mathrm{a}}) + \rho_{\mathrm{b}} E_{\mathrm{a}} t_{\mathrm{a}} E_{\mathrm{s}} t_{\mathrm{s}} \right] \omega^2$$
$$+ \frac{t_{\mathrm{b}}}{4} \frac{\hat{G}_{\mathrm{a}} \hat{G}_{\mathrm{s}}}{t_{\mathrm{g}}^2} \left(E_{\mathrm{a}} t_{\mathrm{a}} + E_{\mathrm{s}} t_{\mathrm{s}} + \frac{\hat{E}_{\mathrm{b}} t_{\mathrm{b}}}{3} \right)$$

$$A_2 = -\left[\rho_b(\rho_a t_a E_s t_s + \rho_s t_s E_a t_a) + \frac{t_b}{4}\frac{\hat{G}_a + \hat{G}_s}{t_g}\rho_a t_a \rho_s t_s\right]\omega^4 + \left[\rho_b\left(\frac{\hat{G}_s}{t_g}E_a t_a + \frac{\hat{G}_a}{t_g}E_s t_s\right) + \frac{t_b}{4}\frac{\hat{G}_a\hat{G}_s}{t_g^2}(\rho_a t_a + \rho_s t_s)\right]\omega^2$$

$$A_0 = -\rho_b\omega^2\left(\rho_a t_a\omega^2 - \frac{\hat{G}_a}{t_g}\right)\left(\rho_s t_s\omega^2 - \frac{\hat{G}_s}{t_g}\right)$$

The twenty unknown coefficients $C_1, \ldots, C_{20}$ are obtained from the system of algebraic equations determined by the boundary and continuity conditions (Eqs. (25)–(31)) after substituting the expected solutions (Eq. (32) and Eqs. (33)–(38)).

Integrating stains ε_a, ε_s and ε_b with respect to x and substituting into the stress–strain relations Eqs. (3) and (4) give the formulae for the shear stresses in the actuator and sensor bonding layers

$$\tau^+ = \frac{\hat{G}_a}{t_g}\sum_{n=9}^{16}\left(\frac{1}{\alpha_a(k_n,\omega)} - 1\right)\frac{C_n}{k_n}\exp(k_n x) \quad x \in (x_2, x_3) \tag{40}$$

$$\tau^- = \frac{\hat{G}_s}{t_g}\sum_{n=9}^{16}\left(\frac{1}{\alpha_s(k_n,\omega)} - 1\right)\frac{C_n}{k_n}\exp(k_n x) \quad x \in (x_2, x_3) \tag{41}$$

The shear stress distribution is responsible for the mechanical coupling between the piezoelements and the beam, and its influence on the active damping effect is significant.

3. Results

Numerical calculations are performed for the simply supported beam of length $l = 380$ mm, width $b = 40$ mm and thickness $t_b = 2$ mm. The parameters of visco-elastic material of the beam are the following: the mass density $\rho_b = 7800\ \mathrm{kg\,m^{-3}}$, Young's modulus $E_b = 2.16 \times 10^{11}$ Pa and retardation time $\mu_b = 10^{-7}$ s which is applied to limit the resonant amplitudes. The sensor/actuator pair is located between $x_2 = 76$ mm and $x_3 = 114$ mm with its centre placed on the fourth mode line. The thickness of the actuator is $t_a = 0.5$ mm and sensor $t_s = 0.4$ mm. It is assumed that the actuator is made of the PZT ceramic (lead–zirconate–titanate) while the sensor material is the PVDF flexible polymer (polyvinylidene fluoride). The electro-mechanical properties of piezoelectric material are listed in Table 1.

The beam is loaded by the harmonic force $F(t)$ of amplitude equal to unity, acting at $x_1 = 75$ mm. According to the concept of active damping the velocity feedback with the gain factor $k_d = 0.05$ s is as-

Table 1
Material parameters

Material parameter	Actuator PZT(G-1195)	Sensor PVDF
ρ (kg m^{-3})	7280	4500
E (N m^{-2})	6.3×10^{10}	2×10^9
d_{31}^a (m/V)	1.9×10^{-10}	–
d_{31}^s (C/N)	–	3.3×10^{-11}
e_{33} (F/m)	–	1.06×10^{-10}

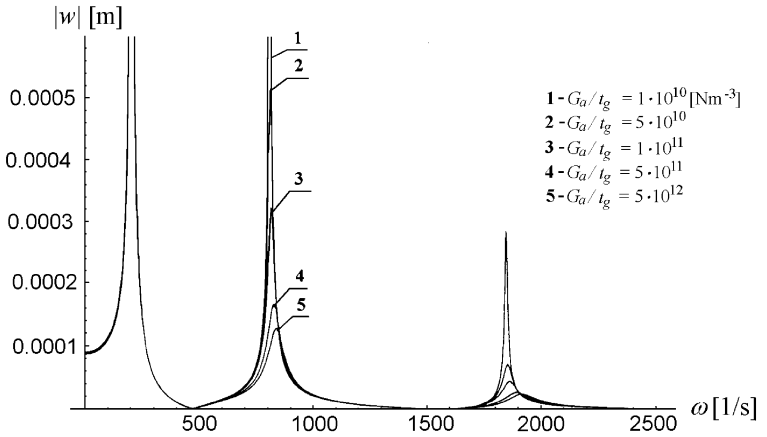

Fig. 3. Effect of variation in the actuator bonding layer stiffness.

sumed. The analysed frequency response functions are calculated at the sensor/actuator field point $x = 90$ mm.

To predict the influence of the bonding layer elasticity on the dynamic response of the controlled beam the calculations are performed for the following values of shearing stiffness parameter $G_j/t_g = 10^{10}$, 5×10^{10}, 10^{11}, 5×10^{11}, 5×10^{12} N m^{-3} (j = a, s). They cover the range from relatively soft to stiff bonding layers.

The results obtained for variations in the stiffness parameter G_a/t_g of the bonding layer between the piezoceramic actuator and the beam are presented in Fig. 3 for a wide range of angular frequencies and in Fig. 4 for the first resonance region. In Fig. 4 the dynamic characteristic referring to the uncontrolled beam is also shown. The stiffness of the sensor bonding layer is assumed constant and equal to $G_s/t_g = 10^{11}$ N m^{-3}. It can be noticed that the amplitudes of the tested vibration modes increase significantly, as the actuator bonding layer becomes soft. This increase is much more expressive at small values of the stiffness parameter G_a/t_g. In addition, the modification of the bonding layer stiffness affects the stiffness of the entire

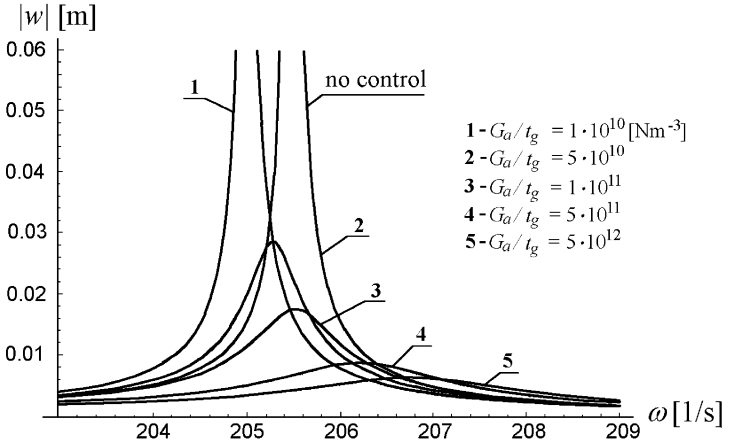

Fig. 4. First mode active damping. Influence of the actuator bonding layer stiffness.

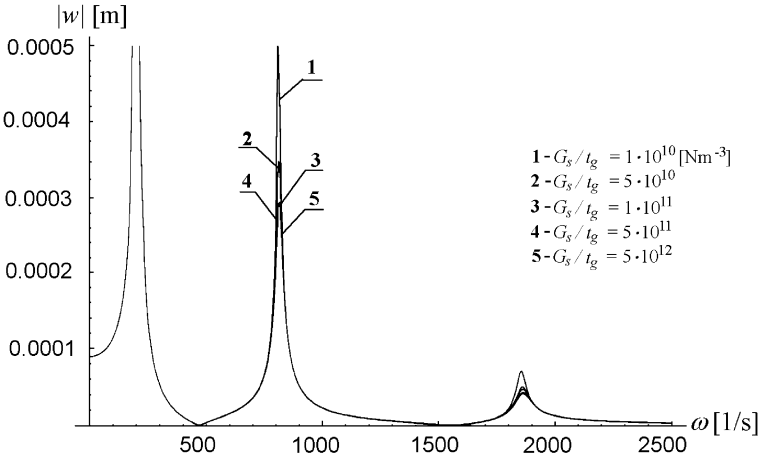

Fig. 5. Effect of variation in the sensor bonding layer stiffness.

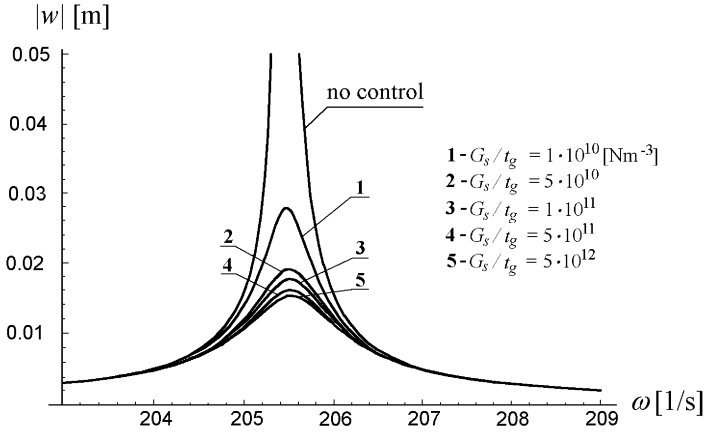

Fig. 6. First mode active damping. Influence of the sensor bonding layer stiffness.

system. One can see that for the soft bonding layer, when a relatively weak coupling between the actuator and the substructure exists, the resonant peaks appear at lower frequencies.

The influence of the stiffness parameter G_s/t_g of the bonding layer between the piezopolymer sensor and the beam is shown in Figs. 5 and 6. The dynamic characteristics presented in Fig. 6 are obtained at the near-first resonance frequencies by supposing a constant stiffness of the actuator bonding layer of the intermediate value $G_a/t_g = 10^{11}$ N m^{-3}. The comparison between Figs. 3–6 show that the effects of variations in both the sensor and the actuator bonding layer stiffness are qualitatively similar. But the system response is less sensitive to variations in the parameter G_s/t_g (see Figs. 5 and 6). In this case the beam deflections at the considered resonance regions do not differ significantly as the sensor bonding layer stiffness alters. The noticeable increase in amplitudes can be observed only for the extremely soft glue layer ($G_s/t_g = 10^{10}$ N m^{-3}). The resonance frequencies are almost independent of the bonding layer stiffness. The reasons of this behaviour of the system are the mechanical properties of the piezopolymer material. The elastic

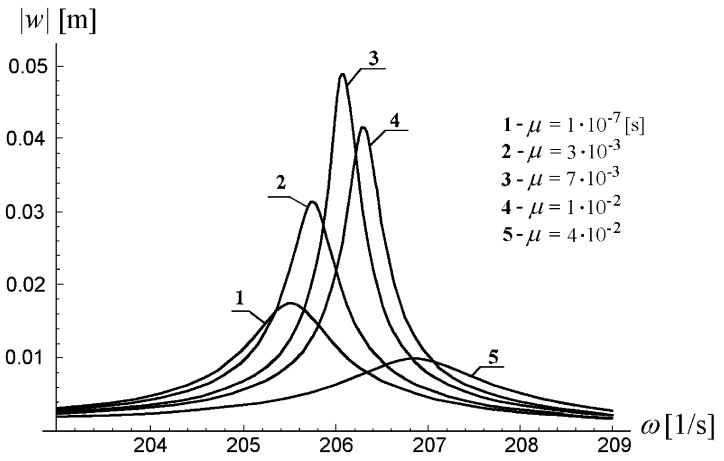

Fig. 7. Effect of material damping in the bonding layers. The first resonance region is tested.

modulus of the PVDF is above 30 times smaller compared with that for the PZT ceramic, and its mass density is also relatively small.

Fig. 7 shows the influence of passive damping in the glue layers on the beam response for the first resonance region. The retardation time μ is assumed to have same value in both the actuator and the sensor bonding layers. Calculations are accomplished for the intermediate shearing stiffness $G_a/t_g = G_s/t_g = 10^{11}$ N m^{-3}. It is observed that the presence of inner damping in the bonding layers causes an increase in the vibration amplitudes of the controlled beam. In the considered case the efficiency of active damping reaches minimum for the retardation time $\mu = 0.007$ s. Some advantage of the glue material damping is only noticed when extremely great values of μ are applied ($\mu = 0.04$ s). As expected, the resonance frequencies become slightly higher with an increase in the bonding layer damping.

Figs. 8 and 9 show the distributions of shear stresses along the actuator and the sensor, respectively, which are induced by the harmonic voltage V_a applied to the actuator. The diagrams are obtained for different values of the bonding layer stiffness by assuming the voltage amplitude $V_0 = 100$ V and almost a static loading, $\omega = 0.1$ s^{-1}. The shear stresses are antisymmetric with respect to the centre of the piezo-element. The distributions of shear stresses transmitted by the actuator depend strongly on the bonding layer stiffness, and change from an approximately linear form for the soft glue layer to the distribution characterised by large stress values concentrated at the ends of the actuator, which refers to the stiff layer. The stress distributions are in a good agreement with the results obtained according to the static analysis presented by Crawley and de Luis (1987). The shear stresses acting on the sensor are almost proportional to the distance from the sensor centre independently of the bonding layer stiffness (see Fig. 9). Only near the sensor ends the increase in shear stresses for the stiff layer becomes significantly greater than that one referring to the soft glue layer.

4. Conclusions

The dynamic model of beam with a collocated sensor/actuator system has been developed by including visco-elastic bonding layers both for the sensor and the actuator. The theoretical analysis and numerical tests are focused on the influence of glue material visco-elastic properties on the active damping of the beam transverse motion. The results presented in terms of amplitude–frequency characteristics show that the

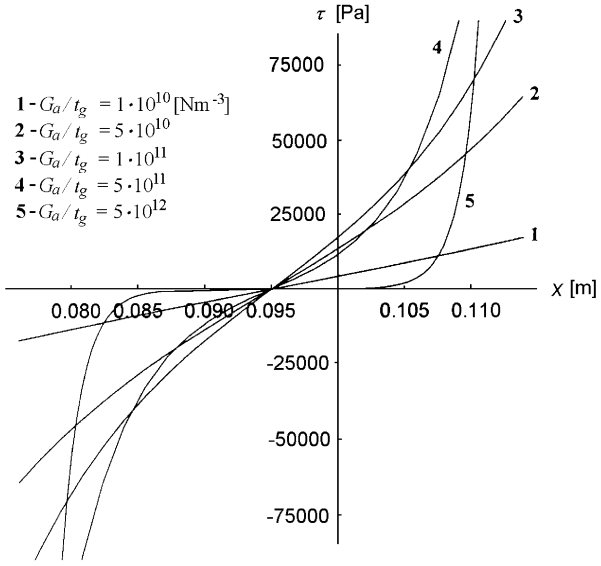

Fig. 8. Shear stress distribution for the actuator at $\omega = 0.1$ s^{-1}.

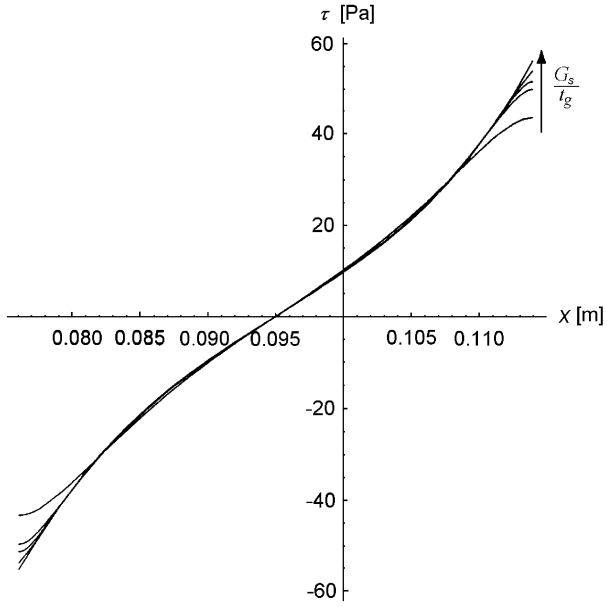

Fig. 9. Shear stress distribution for the sensor at $\omega = 0.1$ s^{-1}.

stiffness of bonding layers affects significantly the active damping efficiency, and they prove the advantage of using relatively stiff bonding layers in the piezoelectric control system. But, it should be emphasised that the sufficiently stiff glue layer increases the hazard of shear stress concentration at the piezoelement ends. Therefore, a damage of coupling between the piezoelement and the basic structure in the form of edge

delamination can be expected. The effects of passive damping (modelled as the Kelvin–Voigt material) are positive, in the aspect of vibration reduction, only for extremely large retardation times. The sensors made of the PVDF polymer do not change the local stiffness of the structure so much, and also decrease considerably the sensitivity of the entire system to visco-elastic parameters of the bonding layers. The lower electro-mechanical constant of piezopolymer material compared with the PZT ceramic can be compensated by an increased gain factor of the feedback loop.

Acknowledgements

This study was supported by the State Committee for Scientific Research (KBN), grant no 7 T07A 04414.

References

Alberts, T.E., Colvin, J.A., 1991. Transfer function analysis for a flexible beam with piezoelectric film actuator and sensor. Proceedings of the Conference on Recent Advances in Active Control of Sound and Vibration, Virginia, pp. 67–77.

Bailey, T., Hubbard, J.E., 1985. Distributed piezoelectric-polymer. Active vibration control of a cantilever beam. Journal of Guidance, Control and Dynamics 8, 605–611.

Crawley, E.F., de Luis, J., 1987. Use of piezoelectric actuators as elements of intelligent structures. AIAA Journal 25, 1373–1385.

Dimitriadis, E., Fuller, C.R., Rogers, C.A., 1991. Piezoelectric actuators for distributed vibration excitation of thin plates. Journal of Applied Mechanics 113, 100–107.

Pan, J., Hansen, C.H., Snyder, S.D., 1991. A study of the response of a simply supported beam to excitation by a piezoelectric actuator. Proceedings of the Conference on Recent Advances in Active Control of Sound and Vibration, Virginia, pp. 39–49.

Lee, C.K., Chiang, W.W., O'Sullivan, T.C., 1991. Piezoelectric modal sensor/actuator pairs for critical active damping vibration control. Journal of Acoustic Society of America 90, 374–384.

Newman, M.J., 1991. Distributed active vibration controllers. Proceedings of the Conference on Recent Advances in Active Control of Sound and Vibration, Virginia, pp. 579–592.

Pietrzakowski, M., 1997. Dynamic model of beam-piezoceramic actuator coupling for active vibration control. Journal of Theoretical and Applied Mechanics 35, 3–20.

Pietrzakowski, M., 2000. Multiple piezoelectric segments in structural vibration control. Journal of Theoretical and Applied Mechanics 38, 35–50.

Tylikowski, A., 1993. Stabilization of beam parametric vibrations. Journal of Theoretical and Applied Mechanics 31, 657–670.

Tylikowski, A., 1999. Stabilization of beam parametric vibrations by means of distributed piezoelectric elements. Journal of Theoretical and Applied Mechanics 37, 241–254.